Microwave heating oxidative stabilization of KMnO4 modified polyacrylonitrile-based carbon fiber precursor

Cheng Zhang
Jianhua Liu (liujianhua501050@163.com)

Research Article

Keywords: Microwave heating, Oxidative stabilization, KMnO4, Modification, Polyacrylonitrile fibers

Posted Date: March 17th, 2021

DOI: https://doi.org/10.21203/rs.3.rs-304764/v1

Abstract

Dielectric property, bulk density, Fourier transform infrared spectroscopy (FT-IR), X-ray photoelectron spectroscopy (XPS), wide angle X-ray diffraction (WAXD), scanning electron microscopy (SEM), energy dispersive spectroscopy (EDS) and mechanical properties were analyzed. PAN fibers (PFs) are polar materials, and the dielectric constant of $KMnO_4$ modification fibers (Mn-PFs) is reduced. The bulk density of Mn-PFs under microwave stabilization (Mn-MSFs) is 0.04 g/cm^3 higher than that of the microwave stabilized fibers (MSFs), shortening the value in one temperature zone. Compared with MSFs5, the stability of Mn-MSFs5 is improved by 10%, and the surface O content and O-containing functional groups are improved. The (002) crystal plane diffraction peak of Mn-MSFs5 is higher than that of MSFs5, and it has a higher stabilized structure. Moreover, after stabilization, the Mn element does not exist on the fiber surface and does not affect the structure of the stabilized fiber. The fineness of Mn-MSFs5 is 1.07 dtex, tensile strength is 1.52 cN/dtex, tensile modulus is 59.3 cN/dtex and elongation at break is 13.5%. It has excellent mechanical properties. In addition, a structural transformation of the thermal stabilization process is proposed, that is, the cyclization reaction first occurs, and then the dehydrogenation and oxidation reactions are performed.

Introduction

Carbon fibers reinforced composite materials are characterized by light weight, high mechanical strength and excellent performance, and are key materials in the 21st century.[1-3] Carbon fiber plays a great role in promoting the national defense and economic development.[4, 5] The global demand for carbon fiber is shown in Fig. 1(a), which is calculated at a growth rate of 10%. The demand for 2020 is expected to be 112.1 kilo-tons.[2, 6] Carbon fibers are mainly classified into PAN $(C_3H_3N)n$, viscose $(C_6H_{10}O_5)n$ and pitch $(C_{124}H_{80}O_{11})n$-based carbon fibers due to the different matrix materials used.[7, 8] Among them, PAN-based carbon fibers occupies about 90% of the use amount with more excellent cost performance.[5, 9] From PFs to carbon fibers, it mainly undergoes three processes of stabilization, carbonization and graphitization.[10, 11] As shown in Fig. 1(b), the stabilization process consumes 48% of energy, which is the most energy-consuming step in the whole production process.[1]. Stabilization is a bridge when organic PFs are converted to inorganic carbon fibers.[12]

Fig. 1. (a) Global demand of carbon fibers, (b) Energy consumption in the production of carbon fibers.

At present, the commercial production of PFs-based carbon fibers is mainly heated by conventional muffle furnaces, which consume large amounts of energy and the fibers easily form defects in the skin-core structure.[13, 14] As a new heating method, microwave energy is a clean energy source that directly heats the material by the energy dissipation inside the material through microwaves.[15] Microwave heating has the characteristics of selective heating, internal heating, non-contact heating, etc. It is easy to control and improve working conditions.[7, 16] The application range of microwave energy has been continuously expanded, and it has been applied in metallurgy, chemical, petroleum, food processing,

medicine and other industries.[12, 17, 18] However, if PFs are heated in a commercial microwave oven, it is necessary to analyze and test the dielectric properties of the fibers. When the dielectric material is illuminated by microwave energy, the material is polarized, resulting in an intrinsic (macroscopic) parameter called relative complex dielectric constant. It denoted by $\varepsilon_\gamma = -j$, Where j is an imaginary unit, $j^2 = -1$, is the relative dielectric constant and is the relative loss factor.[19, 20] The polar substance has a dielectric constant greater than 3.6, weakly polar material between 2.8 and 3.6, and a non-polar material less than 2.8. For the heating process, the better parameter describing the latter is the loss tangent, tanδ = / .[21] Especially the loss factor is related to the frequency, so the heat generated in the material has a function relationship with the frequency.[22] Therefore, it is necessary to understand the relationship between dielectric constant and frequency in order to improve the microwave-assisted heating process.

Microwave heating addresses the problem of heat transfer in conventional oxidation stabilization.[8] while the problem of mass transfer in conventional heating exists. The purpose of the modification process is tantamount to solving the mass transfer problem of the process. Studies have shown that it is necessary to modify PFs for pre-oxidation before the stabilization process in order to shorten the stabilization time and lower the temperature.[23, 24] The nature of the modification is to change the orientation of the molecular chain, control the temperature and time and then affect the stability of the cyclization reaction. Reduces melting and adhesion between fibers to improve mechanical properties and optimize the stabilization process[25] In the modification process, commonly used strong oxidants are H_2O_2,[26-28] $KMnO_4$,[9, 23, 29] and $KClO_3/H_2SO_4$.[30] In the author's research on KMnO4 modified PFs, the optimal modification concentration of $KMnO_4$ is 2 wt.%. The optimal processing temperature and time are 80 °C and 30 min, respectively.

In this study, the PFs was modified with $KMnO_4$ and the oxidative stabilization of the Mn-PFs were carried out under microwave heating. The fiber of different stages was analyzed by dielectric property, bulk density, chemical structure (FT-IR), surface chemical composition (XPS), crystal structure (WAXD), microscopic structure (SEM), elemental content (EDS) and mechanical properties.

Experiments

The inherent and macroscopic parameters of the dielectric constant are related to the physical, chemical composition and frequency of the material. Moreover, the dielectric properties of powder samples were measured using the resonant cavity perturbation method.[20, 31] Therefore, the dielectric properties of the fiber can be obtained by the resonant cavity perturbation method. The principle is to measure the resonance frequency and quality factor before and after the fiber is loaded, so that the dielectric constant is calculated based on the difference between the resonance frequency and the quality factor. In our work, the dielectric properties of PFs and Mn-PFs were heated from room temperature to 300 °C in a resonant cavity at intervals of 50 °C and a frequency of 2450 MHz. The fibers were cut into pieces and placed in a single-mouth quartz tube having an inner diameter of 3 mm, an outer diameter of 5 mm, and a length of 50 mm, and the nozzle was sealed with asbestos. The fiber-filled single-mouth quartz tube was placed in

a glass tube having an inner diameter of 8 mm, an outer diameter of 10 mm, and a length of 500 mm, and the quartz tube was raised and lowered by an air pump.

The schematic diagram of the dielectric property measuring instrument is illustrated in Fig. 2. It consists of cylindrical resonant cavity, control system, dielectric tester, coupling device, water cooler, temperature controller, induction heating equipment and air compressor.

Fig. 2. Schematic diagram of dielectric test system.

Fiber is made of polyacrylonitrile copolymerized with 98.5% acrylonitrile (AN) and 1.5% itaconic acid (IT). PFs (12 K) are supplied by SINOPEC Shanghai Research Institute of Petrochemical Technology, China. Acetone and $KMnO_4$ were purchased from Shanghai Aladdin Biochemical Technology Co., Ltd., China.

Schematic diagram of the modification process and microwave oxidation stabilization is shown in Fig. 3. The modification process was performed in a constant temperature water bath with a stirring speed of 30 r/min. The concentration of $KMnO_4$ was 2 wt.%. The solution temperature was 80 °C and the treatment time was 30 min. The Mn-PFs were subjected to a temperature zone heating treatment in a self-made microwave oven, and the temperature was raised from a gradient of 180 °C to 260 °C at intervals of 20 °C. Microwave power is 960 W, holding time is 5 min, and heating rate is 2 °C/min.

Fig. 3. Schematic diagram of the modification process and oxidative stabilization.

Results And Discussion

The bulk density of the fibers was measured by the sink-float method. Several measurements were made for each fiber sample until the standard deviation value < 0.005. The chemical structural changes of the fibers were examined by FT-IR of model Nicolet iS50. The extent of reaction (EOR) of the stabilized fibers is calculated by Equation 1: **See equation 1 in the supplementary files.**

where $I_{C=N}$ and $I_{C\equiv N}$ represent the strength of the absorption peaks of the fibers at 1580 ($\delta_{C=N}$) and 2240 cm^{-1} ($\nu_{C\equiv N}$), respectively. The binding energy was determined via multi-functional scanning imaging photoelectron spectroscopy (XPS, PHI5000 Versaprobe-II, Japan) by using a 15 kV/50 W monochromatic Al Kα X-ray source. The linear background was subtracted using spectral analysis software (Peak-Fit) and the XPS data was fitted using the Gaussiane-Lorentzian peak shape. The crystal structure was studied using WAXD (TTR18, Japan) with CuKα radiation, where λ is 1.5418 Å, voltage is 40 kV and current is 40 mA. Test process scan from 5° to 50° at 2 °/min. The surface morphology of the fibers were observed by SEM of model XL30ESEM. The mechanical properties of the fibers were tested using a UTM testing machine.

In microwave field, the heating effective of the material by the microwave depends on the ability of the material to respond to the microwave.[33] Therefore, the determination of the dielectric properties of PFs is helpful to study the oxidation stabilization process of microwave-heated PFs. In Fig. 4(a), (dielectric

constant) increases with increasing temperature, PFs rise from 6.638 to 6.813, and Mn-PFs rise from 6.498 to 6.656. The modified fiber has a lower value than unmodified, but both values are greater than 3.6. One possible cause of this is that during the $KMnO_4$ modified fiber process, MnO_4–C=N is formed by –MnO_4 and C≡N, thereby changing the dielectric properties. In Fig. 4(b), before 100 °C, (dielectric loss factor) decreases with increasing temperature and gradually increases after 100 °C. At 300 °C, the PFs is 10.24×10^{-2} and the Mn-PFs is 9.157×10^{-2}. In Fig. 4(c), before 100 °C, tanδ (dielectric loss tangent) decreases with increasing temperature and gradually increases after 100 °C. The tanδ of PFs is lower than Mn-PFs before 250 °C. It may be that the fibers have been completely oxidized and stabilized, during which cyclization, dehydrogenation and oxidation processes have taken place. At 300 °C, the PFs is 1.5×10^{-2} and the Mn-PFs is 1.38×10^{-2}. According to the above analysis, the PFs has good dielectric properties, and the responsiveness of the modified fiber to microwave is lowered.

Fig. 4. Dielectric properties of PFs and Mn-PFs: (a) , (b) , (c) tanδ.

The bulk density of the fibers is shown in Fig. 5. The bulk density of PFs is 1.180 g/cm^3, and the bulk density of Mn-PFs does not change. At the same temperature zone, the bulk density of Mn-MSFs is always higher than that of MSFs. Mn-MSFs5 is 1.371 g/cm^3, which is 0.04 higher than that of MSFs5. It can be seen that the degree of stabilization of the modified fiber is increased by one temperature zone compared to the unmodified fibers.

Fig. 5. Bulk density of different fibers.

FT-IR spectral analysis is shown in Fig. 6. In Fig. 6(a), $KMnO_4$ has a main absorption peak at 1735 and 883 cm^{-1}. In the PFs, there are mainly absorption peaks of 2924 ($\nu_{C\text{-}H}$ in CH_2), 2240 ($\nu_{C\equiv N}$ in CN), 1455 ($\delta_{C\text{-}H}$ in CH_2), 1360 ($\delta_{C\text{-}H}$ in CH) and 1070 cm^{-1} ($\nu_{C\text{-}C}$). A new peak at 2340 cm^{-1} was found in the Mn-PFs, which is a new structure MnO_4–C=N formed by the combination of –MnO_4 and C≡N. This is consistent with Ko, T.H in the study of $KMnO_4$ modified PAN precursors [29] and our previous studies.[9] The changes of chemical structure are shown in Fig. 6(b). Due to the decrease of C≡N and the increase of C=N, the absorption peak intensity of 2240 cm^{-1} is weakened and the absorption peak at 1624 cm^{-1} is enhanced compared with PFs. It further proves that –MnO_4 grafts in PFs.

The functional group change from the PFs to the stabilizing fiber clearly indicates that the oxidative stabilization process undergoes cyclization, dehydrogenation and oxidation reactions. These reactions are closely related to the further formation of a ladder structure by the PFs.[34] After stabilization, the peak corresponding to 2924, 2240, 1455, 1070 cm^{-1} functional group almost disappears, and a sharp peak appears at 1580 cm^{-1}, indicating that the oxidation stabilization process has completely proceeded. Among them, it is obvious that the C=N peak intensity at 1580 cm^{-1} increases gradually before Mn-MSFs3. There is no significant change after Mn-MSFs3, indicating that a cyclic structure is formed in the molecular chain. In contrast, the C=C–H peak intensity at 802 cm^{-1} does not change before Mn-MSFs3, indicating that no dehydrogenation reaction occurs. After that, the peak intensity gradually weakens, and

a dehydrogenation reaction occurs to lose hydrogen. Based on the above analysis, we propose that during the microwave heating of Mn-PFs, the cyclization reaction occurs first, followed by the dehydrogenation reaction.

The EOR of the stabilized fibers are calculated by Equation 1 and the result is shown in Fig. 6(d). MSFs1 is 0.330, Mn-MSFs1 is increased by 0.157. The EOR value of Mn-MSFs5 is 0.783, which is nearly 10% higher than the oxidation stability of MSFs5.

Fig. 6. (a) FT-IR spectra of $KMnO_4$, PFs and Mn-PFs, (b) Modification of $KMnO_4$, (c) FT-IR spectra of Mn-MSFs, (d) EOR.

XPS is an electronic spectroscopy (ESCA) for chemical analysis, a unique technique for atomic element information that captures the molecular structure of fiber surface.[35] As shown in Fig. 7, the XPS spectrum shows significant carbon (C1s 284.8 eV) and oxygen peak (O1s 532.1 eV), representing the major components of the fibers.[36] $KMnO_4$ has strong oxidizing properties, and the O element content of Mn-PFs is higher than that of PFs. O content in Mn-MSFs1 and Mn-MSFs2 does not change significantly, indicating that the cyclization reaction first occurred. During the stabilization process, the content of the O element is first lowered and then increased. Since the dehydrogenation reaction consumes O, it lowers. An oxidation reaction occurs, O_2 in the air enters, so that O increases. In addition, the O content of Mn-MSFs5 is higher than that of MSFs5, which also indicates that the degree of oxidation stabilization improves by microwave after modification.

Fig. 7. XPS wide scan spectra of different fibers.

Variations in fibers of functional groups are considered a measure of the treatment effect. Fig. 8 is a carbon-based surface functional group having different binding energy obtained from the C1s peak of the fibers. C1s peak can be fitted to three Gaussian peaks assigned to C–C of 284.8 eV, C–O–R of 286.4 eV and –C=O of 287.9 eV.[37] As a result, the C1s functional group composition of different fibers samples are shown in Table 1. Mn-MSFs1 and Mn-MSFs2 mainly contain C–C and C–O–R functional groups because the oxidation reaction is not carried out at the initial stage of stabilization. As the stabilization progresses, a –C=O functional group appears. Mn-MSFs5 has a higher content of O-containing groups than MSFs5.

Fig. 8. C1s peak fitting for the fibers (a) Mn-MSFs1; (b) Mn-MSFs2; (c) Mn-MSFs3; (d) Mn-MSFs4; (e) Mn-MSFs5; (f) MSFs5.

Table 1 Functional group compositions of fibers.

Fig. 9 shows the WAXD pattern of the fibers in different states. The particularity of PFs is that there are only two major diffraction peaks 2θ = 17° (100) and 29°(110).[38, 39] After the modification, the absorption peak of Mn-PFs is weakened relative to PFs. As the temperature increases, the 2θ = 17° and 29° absorption peaks gradually decrease. However, compared with 2θ = 17°, 2θ = 29° disappears first. After

stabilization, an absorption peak of the (002) crystal plane appears at 2θ = 25.5°. Moreover, in the carbonization process, the diffraction peak at this point increases as the carbonization temperature increases. At this time, the diffraction peak of Mn-MSFs5 at 2θ = 25.5° is higher than that of MSFs5, and it can be explained that the degree of oxidation stabilization is superior.

Fig. 9. WAXD diagram of fibers in different states.

The surface topography of the fibers and their elemental composition is shown in Fig. 10. In Fig. 10 (a), the "groove" comes from the spinning process. And the "grooves" are the most direct form of fibril. Surface scanning results shows that there are mainly four elements of C, N, O and Si on the surface of PFs, of which C and N elements occupy about 90% of the total. From Fig. 10 (b), it is observed that white crystals exist on the surface of Mn-PFs, which indicates that $KMnO_4$ exists on the fiber surface. The weight content of Mn element in energy spectrum data is 2.86%, and O element is 24.35%. After modification, O content on the fiber surface was increased. During oxidative stabilization, cyclization, dehydrogenation, and oxidation reactions occur, and the fiber structure becomes tighter, which reduces the surface "grooves" of Mn-MSFs5 and MSFs5. The diameter of Mn-MSFs5 is significantly smaller than that of MSFs5, indicating that it has a higher degree of stabilization. The absence of Mn element on the surface of Mn-MSFs5 indicates that the structure of the stabilized fibers is not affected after the stabilization treatment. The above conjecture was confirmed again, $-MnO_4$ and the fiber formed a MnO_4–C=N structure, and the structure disappeared after the cyclization reaction, followed by dehydrogenation and oxidation reactions.

Fig. 10. SEM of fibers: (a) PFs, (b) Mn-PFs, (c) Mn-MSFs5, (d) MSFs5.

Fig. 11 (a) shows the fineness of fibers. The fineness of PFs is 0.80 dtex, Mn-PFs is increased by 0.03. During the stabilization, Mn-MSFs1 is 0.85, and the fineness is gradually increased. Finally, Mn-MSFs5 is 1.07 dtex, while MSFs5 is 1.05 dtex. The tensile strength of the fibers is shown in Fig. 11 (b). The tensile strength of the PFs is 6.95 cN/dtex, and the Mn-PFs is 6.71 cN/dtex. During the stabilization, the Mn-MSFs1 is 5.13 cN/dtex, and the tensile strength is decreased. Further, the tensile strength of Mn-MSFs5 is 1.52 cN/dtex, and the MSFs5 is 1.61 cN/dtex. The cyclization reaction consumes a large amount of cohesive energy between the molecular chains, which causes the tensile strength of the fibers to decrease during the stabilization process. Oxidative stabilization destroys the orientation and crystal structure, forming an ordered ladder structure.[40] Fig. 11 (c) shows the tensile modulus of the fibers, the modulus of PFs is 131.3 cN/dtex, and the Mn-PFs is reduced to 112.1 cN/dtex. After oxidative stabilization, Mn-MSFs1 is 98.4 cN/dtex and Mn-MSFs5 is 59.3 cN/dtex. However, the tensile modulus of MSFs5 is 76.9 cN/dtex. The oxidative stabilization process is essentially a cross-linking process between molecules, leading to the formation of a network.[41] The elongation at break of the fibers is shown in Fig. 11 (d), with a PFs of 11.6% and an increase in Mn-PFs of 13.3%. The elongation at break is gradually weakened throughout the oxidation stabilization process, with Mn-MSFs1 being 17.1% and Mn-MSFs5 being 13.5%. The elongation at break of MSFs5 is higher than Mn-MSFs and it is 14.6%. Due to the complex molecular chain reaction in this process, the fineness of the fiber increases with the temperature zone, while the

tensile strength, tensile modulus and elongation at break show opposite trends. In summary, Mn-MSFs5 had better mechanical properties than MSFs5.

Fig. 11. Mechanical properties of fibers: (a) Fineness, (b) Tensile strength, (c) Tensile modulus, (d) Elongation at break.

During the thermal stabilization stage, three chemical reactions are generally thought to occur within the fibers: cyclization, dehydrogenation, and oxidation reactions. Morita[42] proposed that the cyclization and dehydrogenation reactions proceed at the same time. This structural transformation image illustrates the connection between cyclization, dehydrogenation, and oxidation reactions, and has been recognized by many scholars.[38, 39, 43] So far, there is still insufficient data to illustrate the sequence between the three reactions. Based on the above experimental analysis, we proposed the structural transformation of the thermal stabilization process of PFs as showed in Fig. 12. During the modification process, $-MnO_4-C=N$ is formed by $-MnO_4$ and $C\equiv N$. At the same time, O atoms enter the interior of the fibers, and in the initial stage of thermal stabilization, a cyclization reaction occurs first, and $-MnO_4$ falls off from $MnO_4-C=N$. The next step is dehydrogenation and oxidation. Finally, a ladder cross-linked structure is formed.

Fig. 12. Chemical reaction mechanism for PFs stabilization.

Conclusion

In this work, we investigated the thermal stabilization of Mn-PFs under microwave heating. PFs are polar materials, and the dielectric constant after modification is weakened. The bulk density of Mn-MSFs is 1.371 g/cm^3, which is 0.04 higher than that of MSFs5. Based on the FT-IR analysis, we propose the sequence of reactions for the stabilization of PFs under this condition, cyclization occurs first, followed by dehydrogenation and oxidation reactions. The EOR value of Mn-MSFs5 is 0.783, which is nearly 10% higher than the oxidation stability of MSFs5. From the XPS analysis, it was found that the O content of Mn-MSFs5 is higher than that of MSFs5, which also shows that the fiber can be modified by microwave heating to improve the oxidation stability. What's more, the composition ratio of O-containing functional groups of Mn-MSFs5 is more than that of MSFs5. The (002) crystal plane diffraction peak of Mn-MSFs5 was higher than that of MSFs5 by WAXD, and it had a higher stable structure. The microstructure shows that after stabilization, Mn element does not exist on the fiber surface and does not affect the structure of the stabilized fibers. Mn-MSFs5 has better mechanical properties.

In summary, modified stabilized fiber has a higher degree of stabilization and mechanical properties. In addition, structural transformation of the thermal stabilization process is proposed. That is, a cyclization reaction occurs first, followed by a dehydrogenation and an oxidation reaction.

Declarations

Acknowledgement

This work was supported by the funds for Construction of high-level talents of Kunming University of Science and Technology (KKKP201763019), Research on Microwave Method in Carbon Fiber Preparation (KKK0201863053) and the Kunming University of Science and Technology Analysis Test Fund (2017T20170001, 2018M20172228010), Yunnan Science and Technology Major Project (Grant No. 2018ZE008, 2018ZE027).

References

1. M. Maghe, C. Creighton, L. C. Henderson, M. G. Huson, S. Nunna, S. Atkiss, N. Byrne, and B. L. Fox, *J. Mater. Chem. A.*, **2016**, 4(42), 16619-16626.
2. C. Wang, K. Xia, H. Wang, X. Liang, Z. Yin, and Y. Zhang, *Adv. Mater.*, **2019**, 31(9), 1801072.
3. J. Y. Cai, J. McDonnell, C. Brackley, L. O'Brien, J. S. Church, K. Millington, S. Smith, and N. Phair-Sorensen, *Mater. Today. Commun.*, **2016,** 9, 22-29.
4. B. A. Newcomb, *Compos. Part A: Appl. Sci. Manuf.*, **2016**, 91, 262-282.
5. M. Sharma, S. Gao, E. Mäder, H. Sharma, L. Y. Wei, and J. Bijwe, *Compos. Sci. Technol.*, **2014**, 102, 35-50.
6. S. Park, H. S. Kil, D. Choi, S. K. Song, and S. Lee, *J. Ind. Eng. Chem.*, **2019**, 69, 449-454.
7. J. Liu, C. Zhang, S. Guo, L. Xu, S. Xiao, and Z. Shen, *Ceram. Int.*, **2019**, 45(1), 1379-1384.
8. J. Liu, S. Xiao, Z. Shen, L. Xu, L. Zhang, and J. Peng, *Polym. Degrad. Stab.*, **2018**, 150, 86-91.
9. C. Zhang, R. Li, J. Liu, G. Chen, S. Guo, L. Xu, S. Xiao, and Z. Shen, *Ceram. Int.*, **2019**, 45(14), 17669-17674.
10. A. Gupta and I. Harrison, *Carbon*, **1996**, 34(11), 1427-1445.
11. A. Gupta and I. Harrison, *Carbon*, **1997**, 35(6), 809-818.
12. C. Zhang, J. Liu, S. Guo, S. Xiao, Z. Shen, and L. Xu, *Ceram. Int.*, **2018**, 44(12), 14377-14385.
13. S. Jin, C. Guo, Y. Lu, R. Zhang, Z. Wang, and M. Jin, *Polym. Degrad. Stab.*, **2017**, 140, 32-41.
14. M. J. Yu, C. G. Wang, Y. J. Bai, Y. Xu, and B. Zhu, *J. Appl. Polym. Sci.*, **2008**, 107(3), 1939-1945.
15. R. Zoughi, P. J. Arias-Monje, J. Gallion, S. Sarkar, P.-H. Wang, P. Gulgunje, N. Verghese, and S. Kumar, *Polymer*, **2019**, 179, 121658.
16. S. Y. Kim, S. Y. Kim, S. Lee, S. Jo, Y. H. Im, and H. S. Lee, *Polymer*, **2015**, 56, 590-595.
17. J. A. Menéndez, A. Arenillas, B. Fidalgo, Y. Fernández, L. Zubizarreta, E. G. Calvo, and J. M. Bermúdez, *Fuel Process. Technol.*, **2010**, 91(1), 1-8.
18. M. Elias, M. K. Amin, S. H. Firoz, M. A. Hossain, S. Akter, M. A. Hossain, M. N. Uddin, and I. A. Siddiquey, *Ceram. Int.*, **2017**, 43(1), 84-91.
19. E. T. Thostenson and T. W. Chou, *Compos. Part A: Appl. Sci. Manuf.*, **1999**, 30(9), 1055-1071.
20. X. Ye, S. Guo, W. Qu, L. Yang, T. Hu, S. Xu, L. Zhang, B. Liu, and Z. Zhang, *J. Hazard. Mater.*, **2019**, 366, 432-438.

21. A. Laybourn, J. Katrib, P. A. Palade, T. L. Easun, N. R. Champness, M. Schröder, and S. W. Kingman, *Phys. Chem. Chem. Phys.*, **2016**, 18(7), 5419-5431.
22. B. Garcia-Baños, J. Catalá-Civera, F. Peñaranda-Foix, P. Plaza-González, and G. Llorens-Vallés, *Materials*, **2016**, 9(5), 349.
23. S. Zargham, S. Bazgir, A. A. Katbab, and A. Rashidi, *e-Polymers*, **2014**, 14(5), 363-372.
24. A. Dongil, B. Bachiller-Baeza, A. Guerrero-Ruiz, I. Rodríguez-Ramos, A. Martínez-Alonso, and J. Tascón, *J. Colloid Interface Sci.*, **2011**, 355(1), 179-189.
25. A. Rasheed, J. Y. Howe, M. D. Dadmun, and P. F. Britt, *Carbon*, **2007**, 45(5), 1072-1080.
26. L. Liu, H. Chen, and D. Pan, *Fiber. Polym.*, **2012**, 13(5), 587-592.
27. Y. Choi, M. Park, H. Kyoung Shin, Y. Liu, J. W. Choi, R. Nirmala, S. J. Park, and H. Y. Kim, *Mater. Lett.*, **2014**, 123, 59-61.
28. C. Zhang, R. Li, J. Liu, S. Guo, L. Xu, S. Xiao, and Z. Shen, *Ceram. Int.*, **2019**, 45(10), 13385-13392.
29. T. H. Ko and C. H. Lin, *J. Mater. Sci. Lett.*, **1988**, **7**(6), 628-630.
30. L. Meng, D. Fan, C. Zhang, Z. Jiang, and Y. Huang, *Appl. Surf. Sci.*, **2013**, 268(3), 225-230.
31. G. He, S. Li, K. Yang, J. Liu, P. Liu, L. Zhang, and J. Peng, *Minerals*, **2017**, 7(2), 31.
32. H. Yuan, Y. Wang, P. Liu, H. Yu, B. Ge, and Y. Mei, *J. Appl. Polym. Sci.*, **2011,** 122(1), 90-96.
33. N. Makul, P. Rattanadecho, and D. K. Agrawal, *Renew. Sust. Energ. Rew.*, 2014, **37**, 715-733.
34. O. Qin, L. Cheng, H. Wang, and K. Li, *Polym. Degrad. Stab.*, **2008**, 93(8), 1415-1421.
35. H. Yuan, C. Wang, S. Zhang, and X. Lin, *Appl. Surf. Sci.*, **2012**, 259, 288-293.
36. F. Cuiqin, W. Jinxian, W. Julin, and Z. Tao, *Appl. Surf. Sci.*, **2015**, 356, 9-17.
37. E. s. Lee, C. h. Lee, Y. S. Chun, C. j. Han, and D. S. Lim, *Compos. Part. B-Eng.*, **2017**, 116, 451-458.
38. N. Hameed, J. Sharp, S. Nunna, C. Creighton, K. Magniez, P. Jyotishkumar, N. V. Salim, and B. Fox, *Polym. Degrad. Stab.*, **2016**, 128, 39-45.
39. M. Ji, C. Wang, Y. Bai, M. Yu, and Y. Wang, *Polym. Bull.*, **2007**, 59(4), 527-536.
40. T. H. H. Elagib, E. A. M. Hassan, C. Fan, K. Han, and M. Yu, *Polym. Degrad. Stab.*, **2018**, 158, 64-71.
41. S. Lei, W. Cao, Z. Fu, and L. Xu, *J. Appl. Polym. Sci.*, **2016**, 133(36).
42. K. Morita, Y. Murata, A. Ishitani, K. Murayama, T. Ono, and A. Nakajima, *Pure Appl. Chem.*, **1986**, 58(3), 455-468.
43. M. S. A. Rahaman, A. F. Ismail, and A. Mustafa, *Polym. Degrad. Stab.*, **2007**, 92(8), 1421-1432.

Table

Table 1 Functional group compositions of fibers.

Samples	Functional group composition (%)		
	C–C	C–O–R	–C=O
Mn-MSFs1	66.33	33.67	–
Mn-MSFs2	70.63	29.37	–
Mn-MSFs3	67.39	25.68	6.92
Mn-MSFs4	70.03	26.26	3.71
Mn-MSFs5	67.69	23.94	8.36
MSFs5	70.29	20.90	8.81

Figures

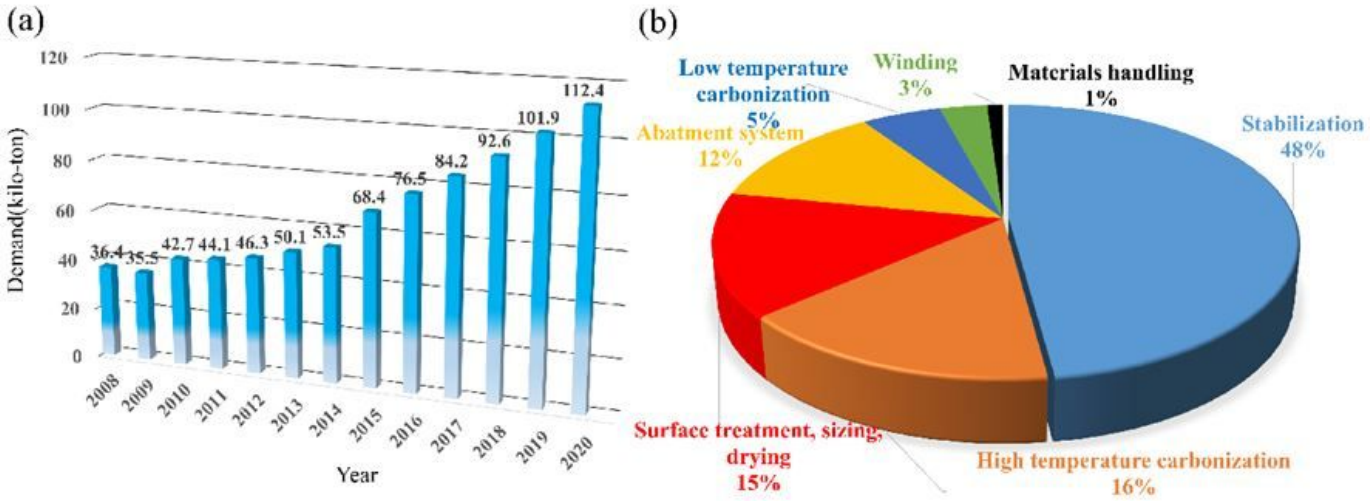

Figure 1

(a) Global demand of carbon fibers, (b) Energy consumption in the production of carbon fibers.

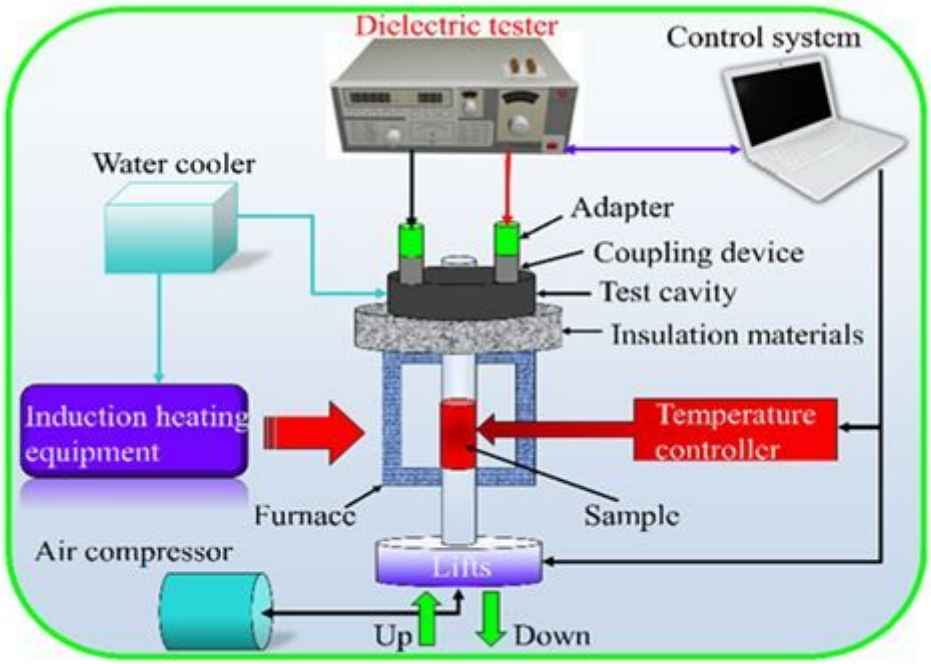

Figure 2

Schematic diagram of dielectric test system.

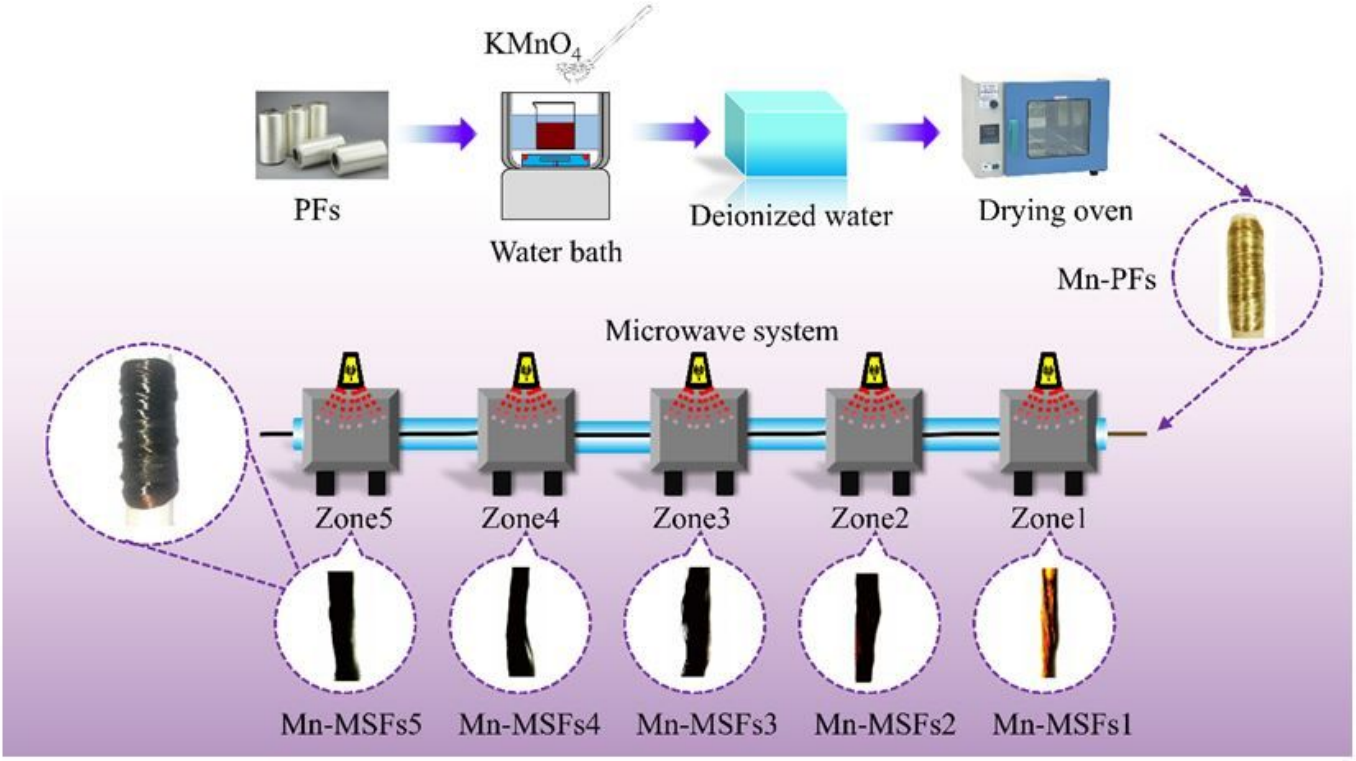

Figure 3

Schematic diagram of the modification process and oxidative stabilization.

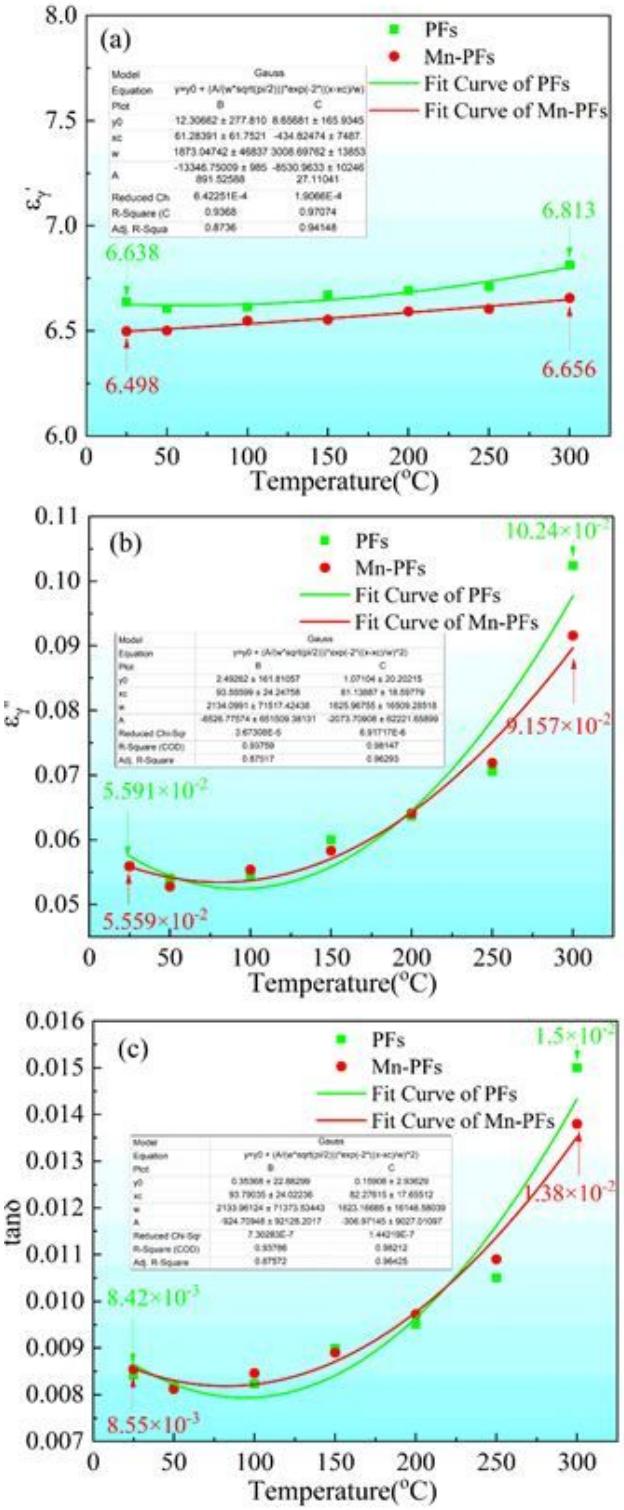

Figure 4

Dielectric properties of PFs and Mn-PFs: (a) , (b) , (c) tanδ.

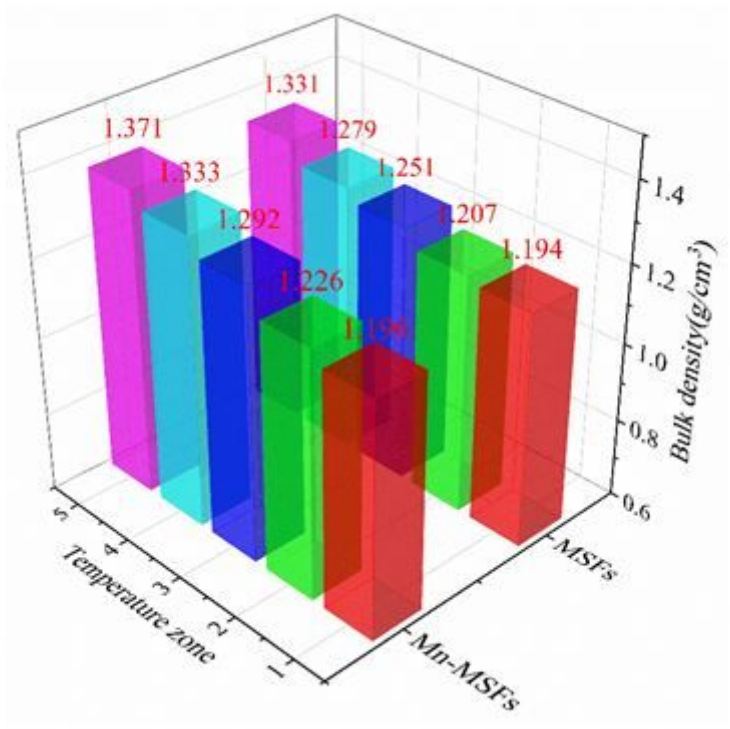

Figure 5

Bulk density of different fibers.

FT-IR spectra of Mn-MSFs, (d) EOR.

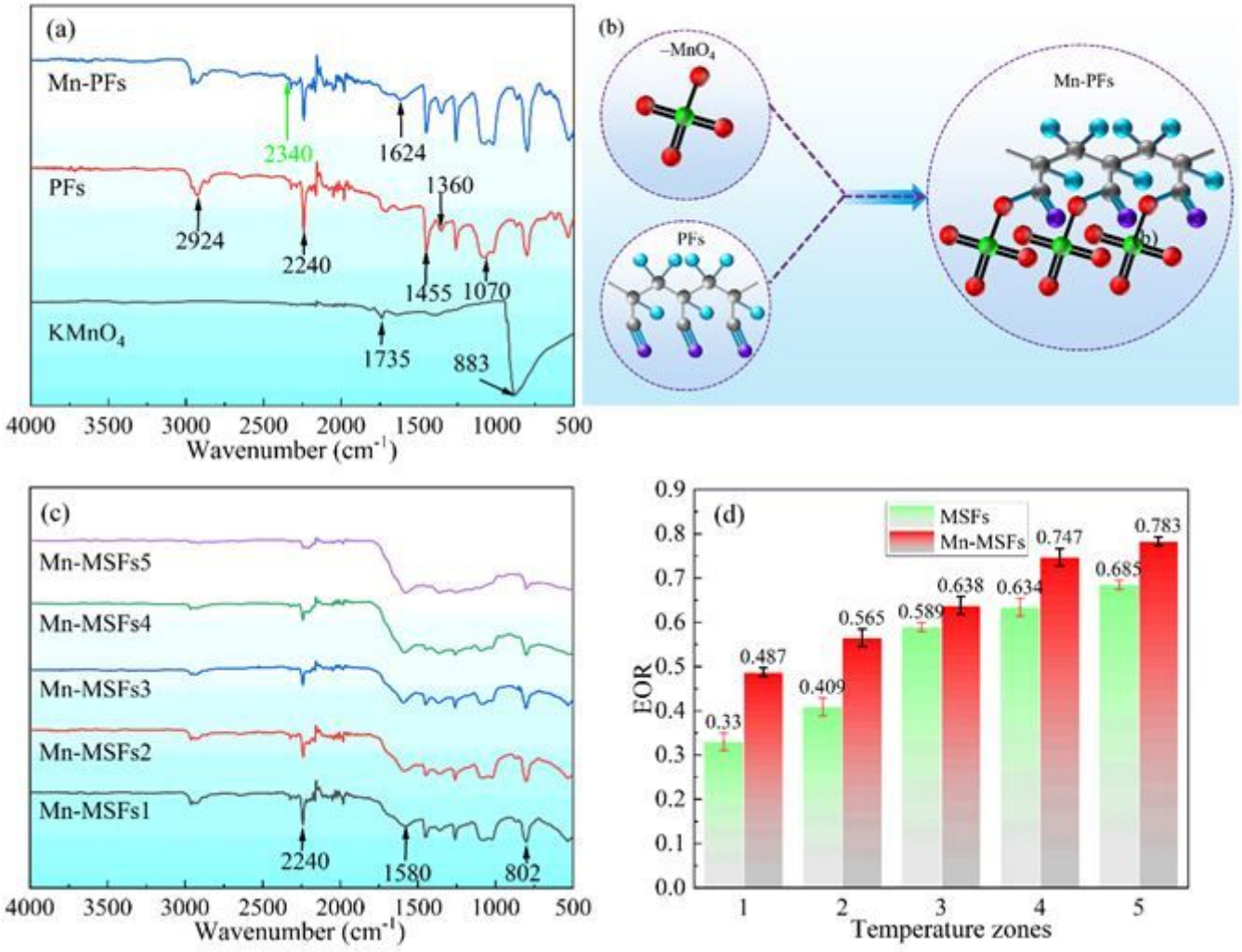

Figure 6

(a) FT-IR spectra of KMnO4, PFs and Mn-PFs, (b) Modification of KMnO4, (c) FT-IR spectra of Mn-MSFs, (d) EOR.

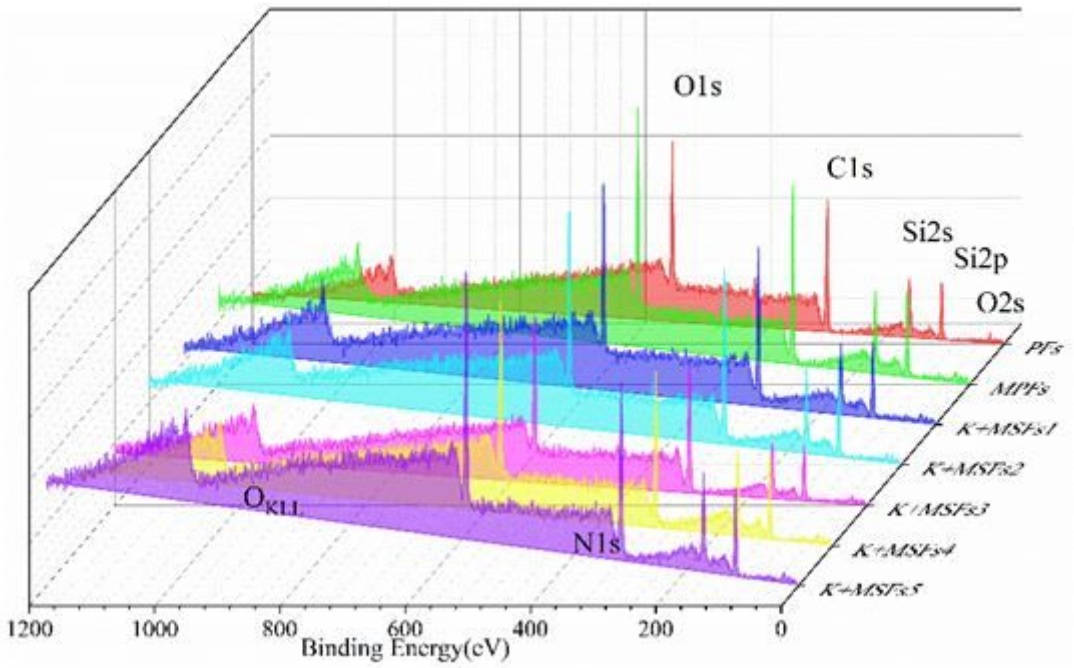

Figure 7

XPS wide scan spectra of different fibers.

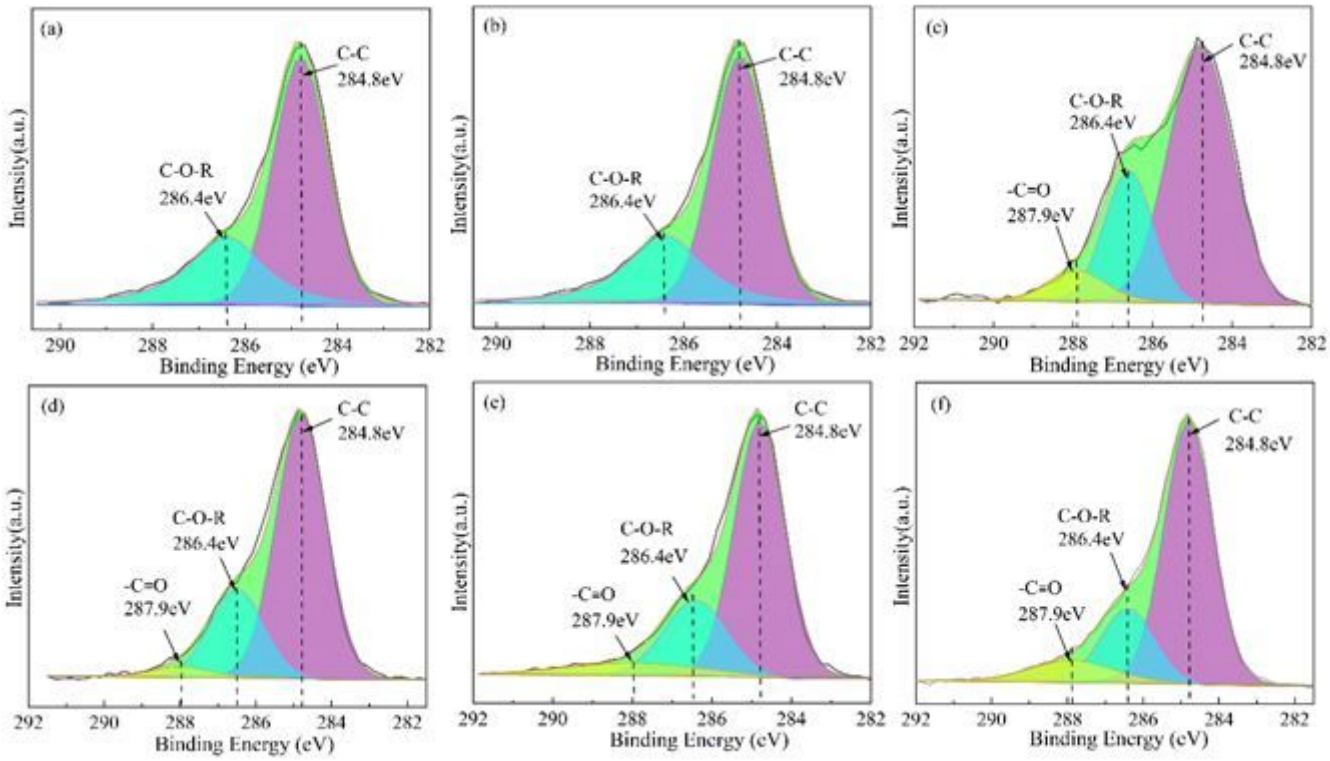

Figure 8

C1s peak fitting for the fibers (a) Mn-MSFs1; (b) Mn-MSFs2; (c) Mn-MSFs3; (d) Mn-MSFs4; (e) Mn-MSFs5; (f) MSFs5.

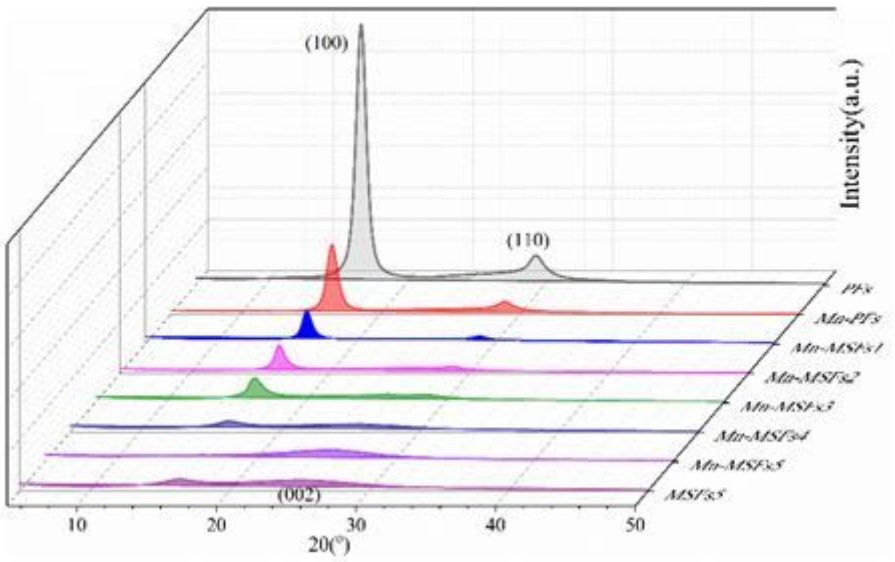

Figure 9

WAXD diagram of fibers in different states.

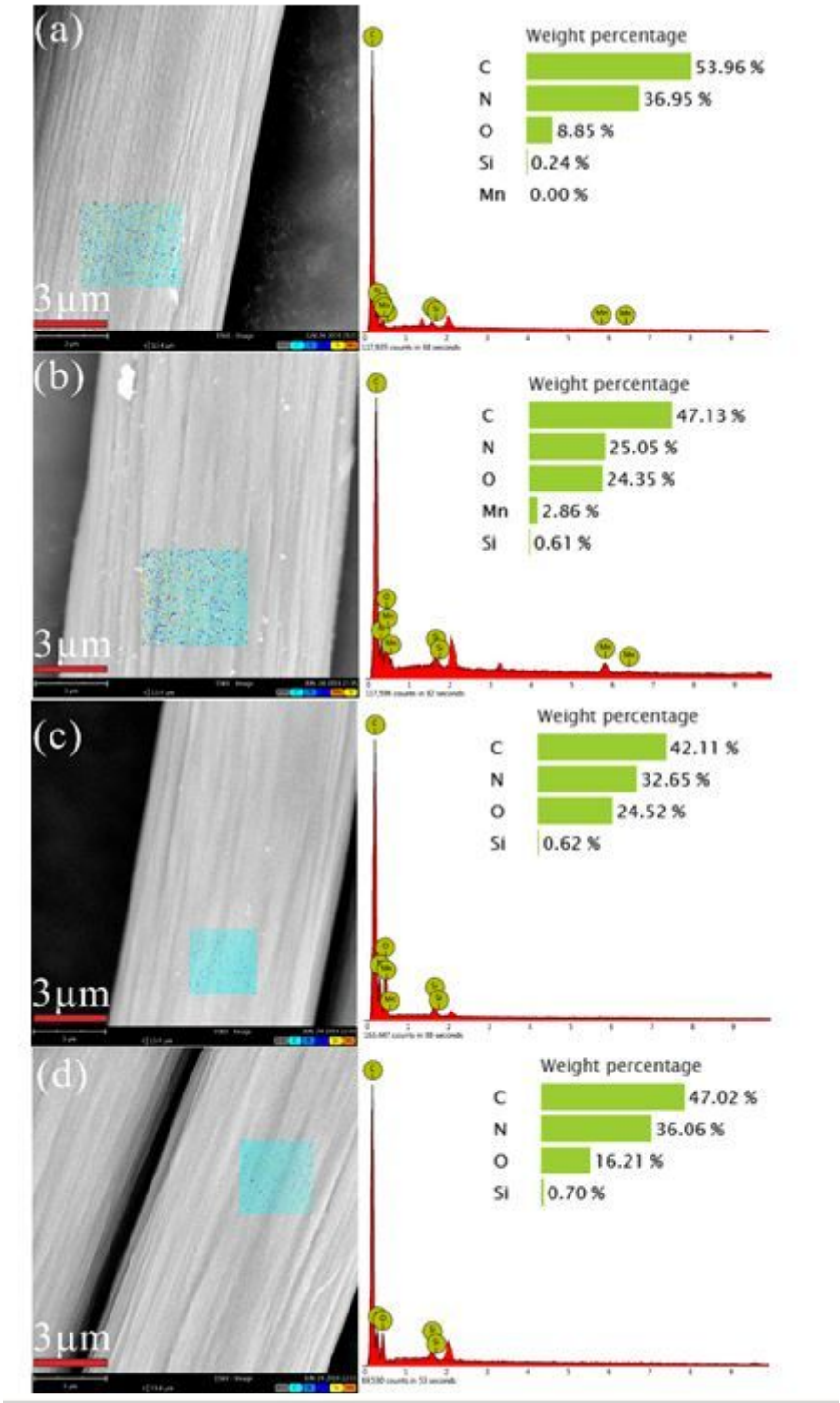

Figure 10

SEM of fibers: (a) PFs, (b) Mn-PFs, (c) Mn-MSFs5, (d) MSFs5.

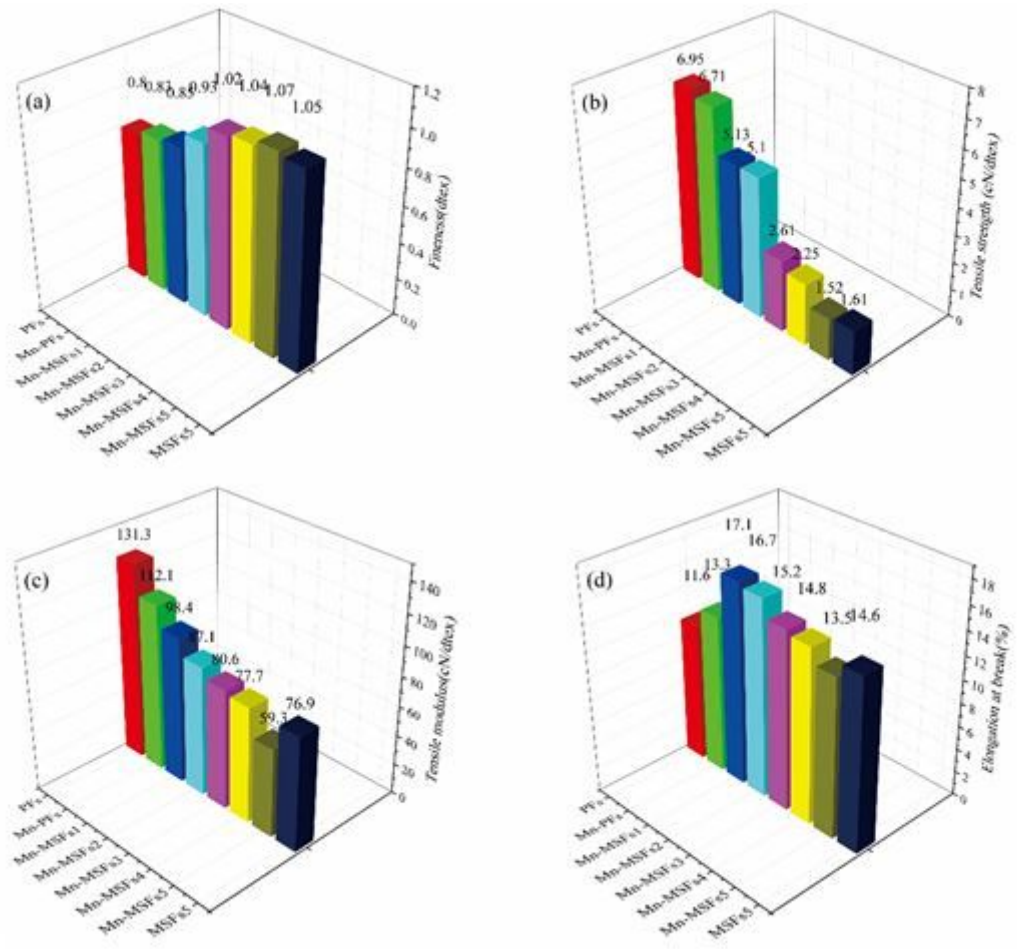

Figure 11

Mechanical properties of fibers: (a) Fineness, (b) Tensile strength, (c) Tensile modulus, (d) Elongation at break.

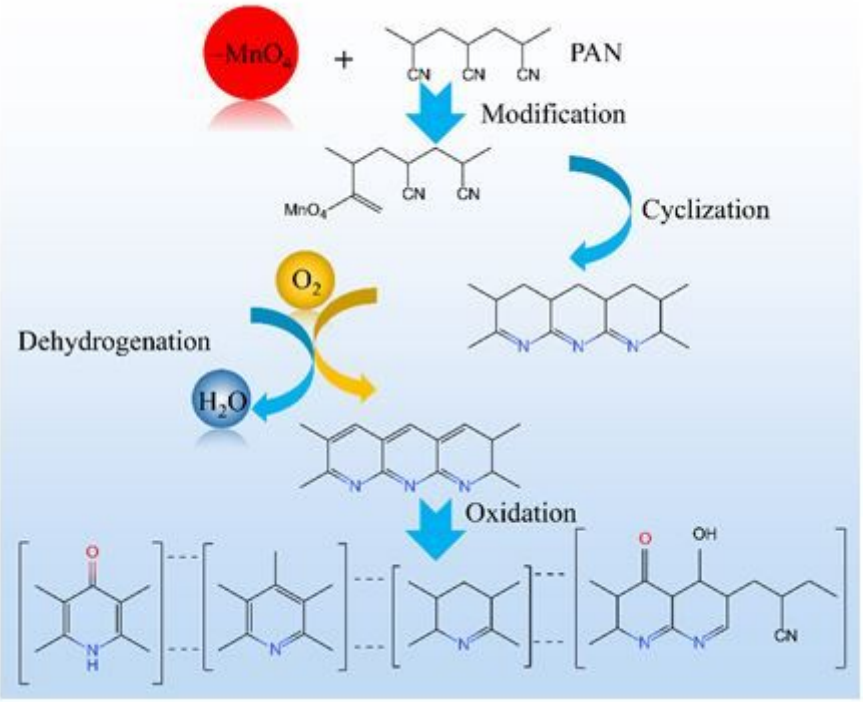

Figure 12

Chemical reaction mechanism for PFs stabilization.